Seismic Performance of Infilled Reinforced Concrete Frame with Crumb Rubber Mortar Wall Panel

Kritsada Chayaboot [1], Maetee Boonpichetvong [1, 2*], Tanyada Pannachet [1, 2], Vanchai Sata [1, 2], Chatpan Chintanapakdee [3, 4]

[1] Department of Civil Engineering, Faculty of Engineering, Khon Kaen University, Thailand.

[2] Sustainable Infrastructure Research and Development Center, Faculty of Engineering, Khon Kaen University, Thailand.

[3] Disaster and Risk Management Information Systems Research Group, Chulalongkorn University, Thailand.

[4] Department of Civil Engineering, Faculty of Engineering, Chulalongkorn University, Thailand

Abstract

In this paper, the seismic performance of reinforced concrete (RC) frames with crumb rubber mortar wall panels is reported. The tests of the crumb rubber mortar were conducted to obtain model parameters for equivalent diagonal compression struts. With a higher percentage of sand replacement by crumb rubber, the unit weight, the compressive strength, the tensile strength, and the modulus of elasticity of the crumb rubber cement mortar are decreased. Nonlinear pushover analysis of a simple frame shows that the RC frame with a wall panel with less crumb rubber demonstrates lower lateral deformation ability. The failure modes are affected by the amount of crumb rubber and are dependent on the modeling choice of the equivalent compression strut as the wall panel representative. Finally, the seismic performance of the RC building was studied by the equivalent static approach to explore the influence of the crumb rubber mortar wall panels on internal forces and deformations of the frame. With a higher percentage of crumb rubber, the weight of the infill wall panels and the overall weight of the building are reduced, which meets lower seismic base shear demand. This benefit is, however, traded off with higher lateral deformation and also higher inter-story drift of the studied building frames.

Keywords: Nonlinear Analysis; Seismic Analysis; Infill Wall Panel; Crumb Rubber; Cement Mortar.

1. Introduction

Handling waste materials is a vital environmental issue that certainly impacts the quality of life in each community. An old car tire is one example that causes environmental concern as it takes a long time to decompose [1], and if incinerated, the generated smoke affects air pollution [2–4]. Unused old car tires from millions of cars draw attention to how to use recycled rubber from these old car tires [5]. In Thailand, the recycling industry manages to cut scrap tires into small crumb rubber, which can be used for many purposes. Application of crumb rubber as a construction material has been explored in the past. Researchers tried to investigate the possibilities of using crumb rubber as a replacement for fine aggregate either in concrete [6–8] or cement mortar [9–12]. It was found that using the crumb rubber obtained from waste tires to replace sand in concrete or cement mortar changed the intrinsic mechanical properties of composites, resulting in a lower compressive strength, a lighter unit weight, and a lower modulus of elasticity [6–12].

Although replacement of sand with crumb rubber in cement mortar or concrete yields a lower weight with a lower strength compound, this recycled construction material may be useful for making lightweight non-structural components of buildings, for example, infill wall panels to be installed in ordinary reinforced concrete buildings. The result of less self-weight acting on a building responds to lower structural force demand for the building structure. The overall construction cost of a building structure can be optimized, especially for the design and construction of buildings subjected to seismic action. As seismic forces induced in a building structure depend on the level of the building weight, the idea of substituting conventional infill walls with much lighter and more flexible walls to reduce the seismic demand of the structure is interesting.

The present literature survey revealed that few studies of crumb rubber concrete were extended to precast wall panels [13–16]. Crumb rubber was reported to enhance sound absorption, thermal insulation [13], and ductility performance [15] of precast concrete panels in comparison with conventional concrete wall panels. The flexural resistance of standard wall panels made of crumb rubber concrete was reported to decrease with increases in rubber aggregate replacement [16]. A recent study [14] reported that improved energy absorption and ductile failure mechanisms could be achieved for rubberized concrete interlocking masonry prisms under axial compression. Although the use of crumb rubber wall panels in the form of crumb rubber concrete and/or crumb rubber mortar was motivated, the published information regarding the seismic performance of building structures installed with crumb rubber wall panels was not available in the present literature [17].

For ordinary reinforced concrete building frame systems, design engineers often neglect the presence of infilled walls and treat infilled walls as non-structural components that do not interact or provide resistance. Such simplification raises no arguments for buildings under the action of gravity but may not be conservative for certain loading conditions, for example, seismic actions. In the past, attempts were made to study the effect of infill walls on reinforced concrete frames under seismic load [18–22]. Under a seismic action, the interaction of the infill walls and the reinforced concrete building frame was shown to affect internal force distribution in the frame [18–20]. The overall building frame was shown to provide larger seismic resistance [23–28], but the interaction between the infill walls and the reinforced concrete frame might yield undesirable failure patterns [21, 29, 30], as the shear failure mode could be observed in some reinforced concrete columns. Modeling the infill walls could be done as a wall continuum model, but this took a computational cost [31]. Inclusion of infill walls together with the reinforced concrete frame for modeling the seismic response of the building during the detailed design was suggested by using diagonal equivalent struts as outlined in several guidelines and standards [32, 33].

The modeling of an infilled wall was often performed by using an equivalent compression strut [32] or multi-strut concept model [34–36]. For the one concentric strut model, the ends of the strut were at the center of column-beam joints [32, 34, 37]. This type of model was used to analyze the overall behavior of a structure [32, 33]. Modeling the strut as one eccentric strut model was recommended [32, 33] to investigate the impact of seismic action on the concerned columns. The one eccentric strut acted on the columns eccentrically from the center of the column-beam joint. The simplest form of a multi-strut concept model is the three-strut model [34, 36, 38], which was observed to resemble well to laboratory test results. In this paper, the infill wall panels that are made of cement mortar with crumb rubber recycled from tire rubber waste were modeled by the one concentric strut [32], the one eccentric strut [32], and the three-strut model [34] to comprehensively study the possible interaction with the reinforced concrete frame subjected to lateral seismic load.

This paper consists of three parts. The first part is the experimental finding of the mechanical properties of the cement mortar using crumb rubber for various mixed proportions. These properties are subsequently translated into model parameters for the inclusion of infill wall panels in the frame using the available diagonal strut models [32, 34, 37–39]. In the second part, in order to gain insight into the lateral resisting mechanism of the studied frame and wall, a nonlinear analysis using the SAP2000 program is performed to study the load-deformation capacity curve. The interaction between the infill wall panel made of cement mortar with crumb rubber and the reinforced concrete building frame in the form of a simple one-bay, one-story model subjected to lateral load is investigated. Finally, the performance of a two-bay, three-story building frame subjected to seismic force is evaluated by means of the seismic equivalent static force method [32, 40, 41]. The methodology is summarized in Figure 1. The objective of this study is to provide the overall building response for the assumed example building that adopts lighter and more flexible infill wall panels made of cement mortar with crumb rubber. The understanding of this work will benefit future development of recycled wall panels made of cement mortar with crumb rubber.
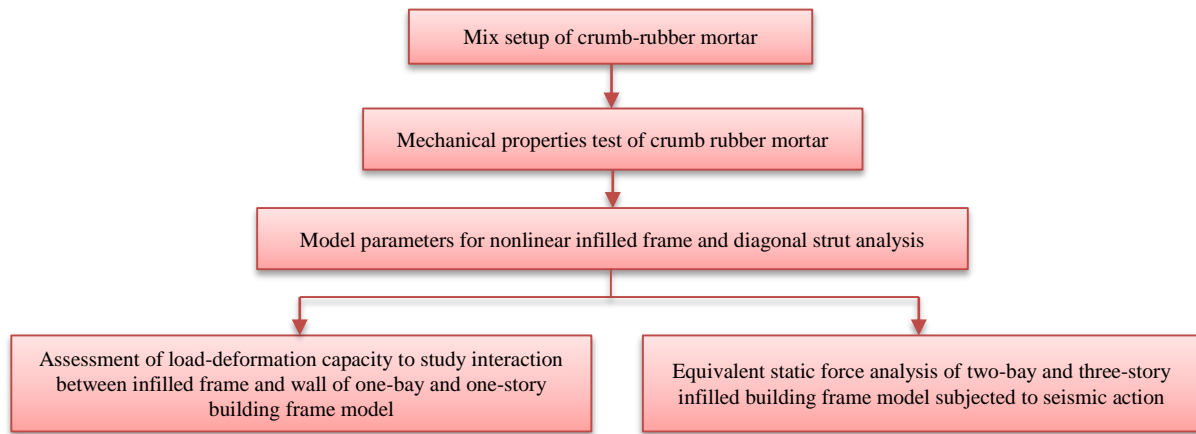
Figure 1. The methodology flowchart

2. Mechanical Properties of Cement Mortar with Crumb Rubber

The basic mechanical properties of the cement mortar, including unit weight, compressive strength, tensile strength, modulus of elasticity, and Poisson's ratio, were determined according to ASTM C109/C109M-01 [42]. In this study, the cement mortar with no sand replacement consisted of a natural sand-to-cement ratio of 2.75 and a water-to-cement ratio of 0.485 by volume. The used sand in this study had a grain size distribution as shown in Figure 2. Waste tires from a local recycled tire industry were used. The used crumb rubber was also sampled and sieved to have the same gradation as the used sand, as shown in Figure 2. The physical characteristics of crumb rubber were found to be wedged, not round, soft, light, and floating. The crumb rubber was used as fine aggregate for sand replacement, so the adopted crumb rubber was selected such that the fineness modulus and the size distribution were close to the properties of natural sand with a fineness modulus of 2.74. The amount of sand in the cement mortar was also varied for sand replacement by crumb rubber at a ratio of 0, 25, 50, 75, and 100 by volume. The mixed proportions for the cement mortar in this study are summarized in Table 1. In total, 30 cylindrical specimens of 10 cm in diameter and 20 cm in height were prepared to determine the compressive strength by the uniaxial compression test and the tensile splitting test according to ASTM C192-19 [43].
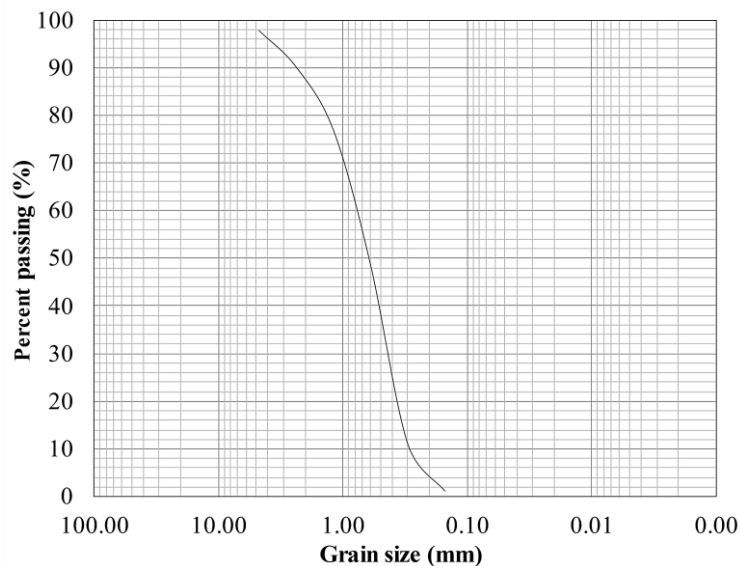

Figure 2. Gradation curve of the used fine aggregate

Table 1. Studied cement mortar mixed with ratio of sand replacement by crumb rubber

Mix	Sand replacement by crumb rubber (% by volume)	
	Sand	**Crumb rubber**
R0	100	0
R25	75	25
R50	50	50
R75	25	75
R100	0	100

2.1. Unit Weight

From the laboratory experiment, the specific gravity of the crumb rubber was found to be 1.22. As the crumb rubber itself was lighter than sand, the unit weight of the cement mortar that was made by replacing sand with the crumb rubber was lower for higher percentages of the crumb rubber volume. The obtained unit weights of cement mortar with crumb rubber are shown in Figure 3.
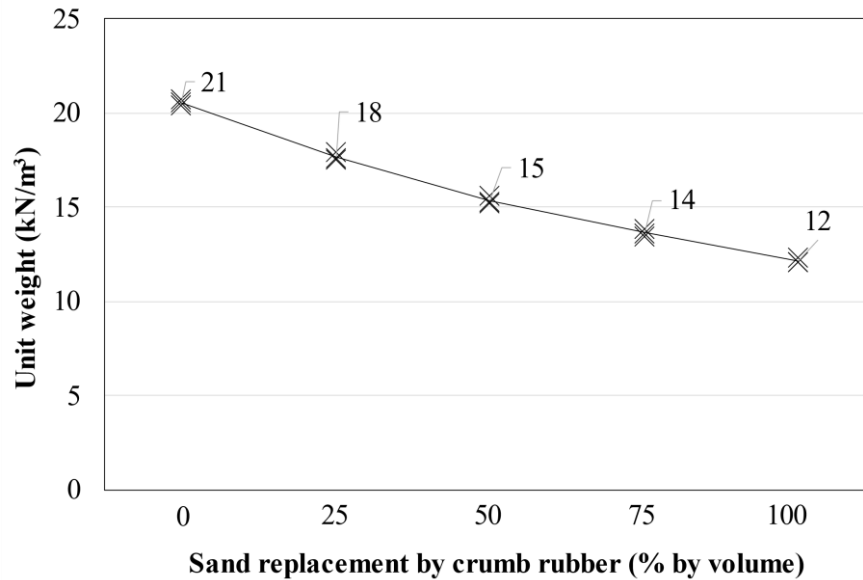

Figure 3. Unit weight of cement mortar with crumb rubber

2.2. Uniaxial Compressive Stress-Strain Relation of Cement Mortar with Crumb Rubber

The uniaxial compression test of the cement mortar with crumb rubber was conducted with measurement of the induced axial and lateral strain as shown in Figures 4 and 5. The results of the stress-strain relation of the studied cement mortar specimens with sand replacement by crumb rubber at 0, 25, 50, 75, and 100% by volume, labeled as mix No. R0, R25, R50, R75, and R100, respectively, are as shown in Figure 6. The positive value of strain shown in the figure represents compressive strain in the axial direction, whereas the negative value of strain indicates the lateral expansion of the specimens.

Figure 4. Uniaxial compression test of cement mortar with crumb rubber specimens

Figure 5. Cement mortar with sand replacement by crumb rubber specimens
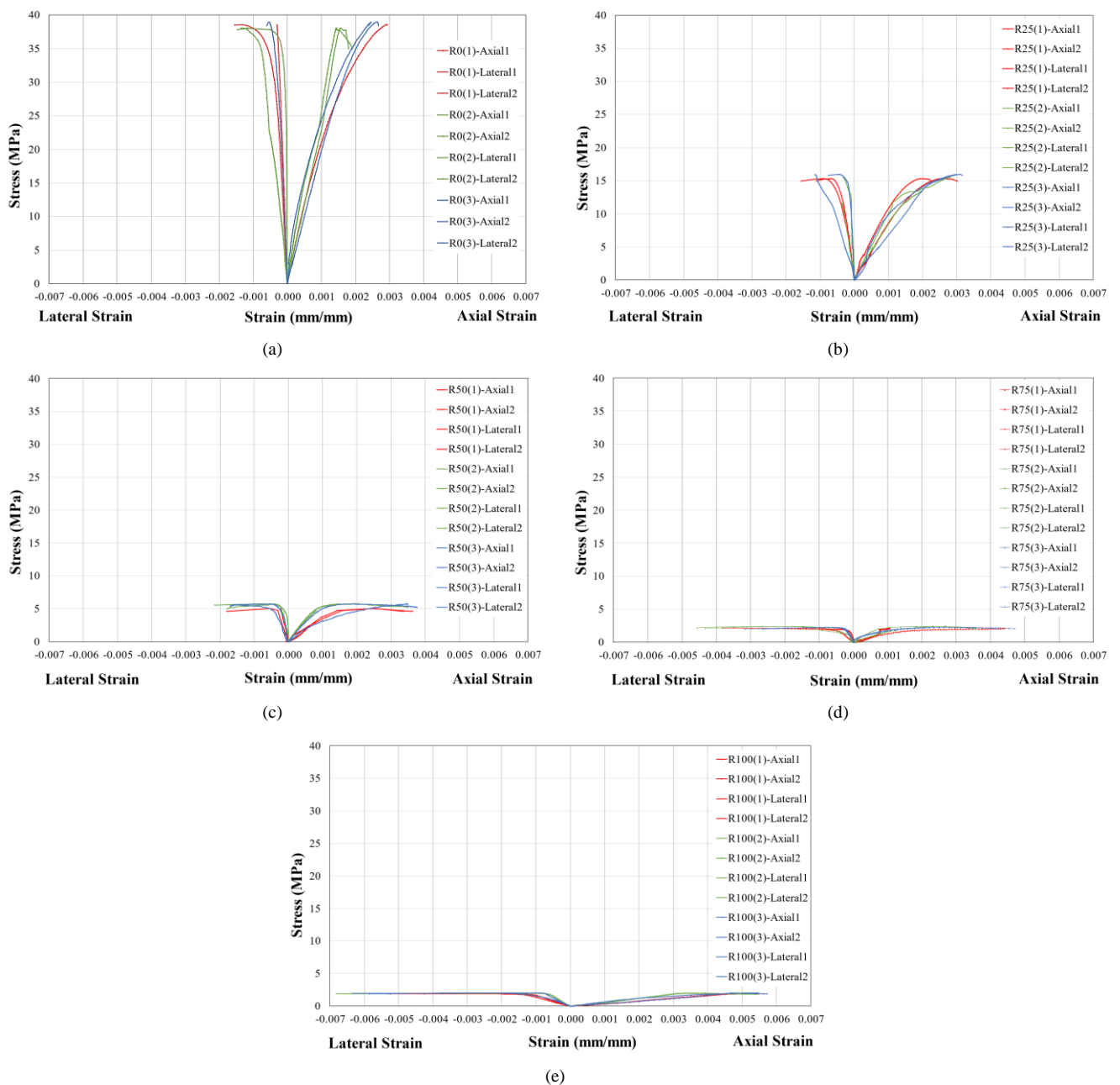

(a)

(b)

(c)

(d)

(e)

Figure 6. Uniaxial compressive stress-strain relation of cement mortar with sand replacement by crumb rubber (a) R0, (b) R25, (c) R50, (d) R75 and (e) R100 specimens

2.3. Compressive Strength and Modulus of Elasticity

The uniaxial compression test of the cement mortar specimens (f_{cm}') was conducted at the age of 28 days. The average compressive strength of the regular cement mortar without crumb rubber was found to be 38.5 MPa. As demonstrated in Figure 7, the compressive strength of the cement mortar with crumb rubber decreases as the volume of sand replaced by crumb rubber increases. Based on the stress-strain relation of the cement mortar with crumb rubber shown in Figure 6, the compressive modulus of elasticity (E_m) of the cement mortar specimens was determined following TMS402 Building Code Requirements for Masonry Structures [44]. As recommended in TMS402, the chord modulus of a straight line connecting two locations on the compressive stress-strain envelope at the stress magnitudes of $0.05 f_{cm}'$ and $0.33 f_{cm}'$ of an infill wall panel can be used to describe the modulus of elasticity of the wall panel under compression, as shown in Figure 8. The compressive modulus of elasticity (E_m) of the cement mortar specimens is summarized in Figure 9. For the normal cement mortar without crumb rubber, the average compressive modulus of elasticity was 24,739 MPa. With increased volume of sand replacement by crumb rubber, the compressive modulus of elasticity was lower. It was observed that replacing sand with the crumb rubber decreased the rigidity of the compound. The level of strain at the compressive strength and the ultimate compressive strain of cement mortar specimens increased with the amount of crumb rubber inclusion. The Poisson's ratios of the cement mortar specimens were in the range of 0.19 to 0.22.
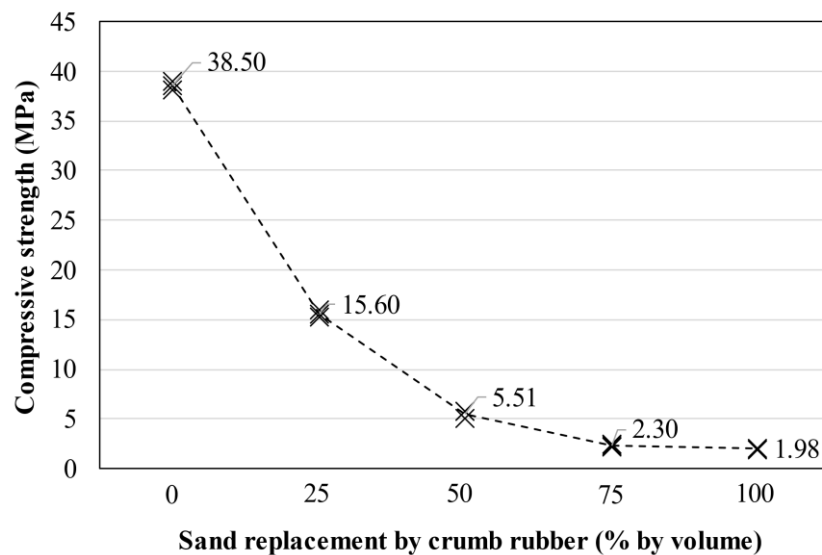

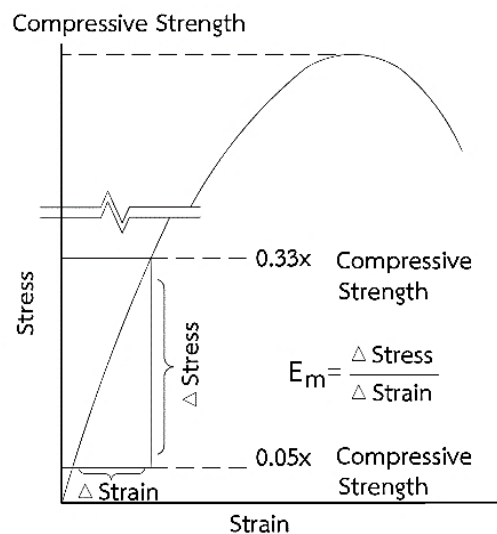**Figure 7. Compressive strength of cement mortar with crumb rubber**

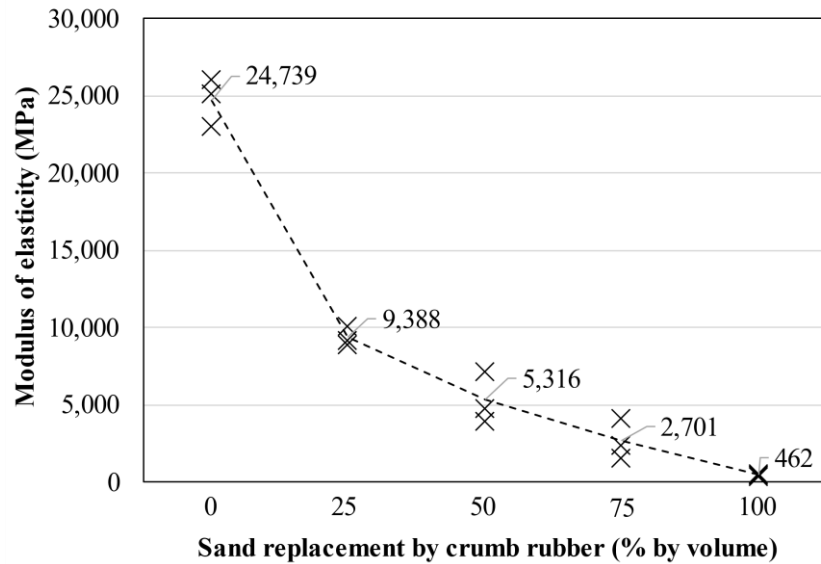**Figure 8. Modulus of elasticity for masonry wall prism [44]**

Figure 9. Compressive modulus of elasticity of cement mortar with crumb rubber

2.4. Tensile Strength

The tensile splitting test of the studied mortar specimens at the age of 28 days was performed as shown in Figure 10. The relation between the tensile strength of the cement mortar with crumb rubber and the amount of crumb rubber is summarized in Figure 11. The average tensile strengths were in the range of approximately 10 to 25 percent of the compressive strength of the normal cement mortar. For the cement mortar specimens with 100 percent sand replacement with crumb rubber (R100), one fourth of the normal cement mortar strength was obtained.

Figure 10. Test of splitting tensile strength of cement mortar with crumb rubber
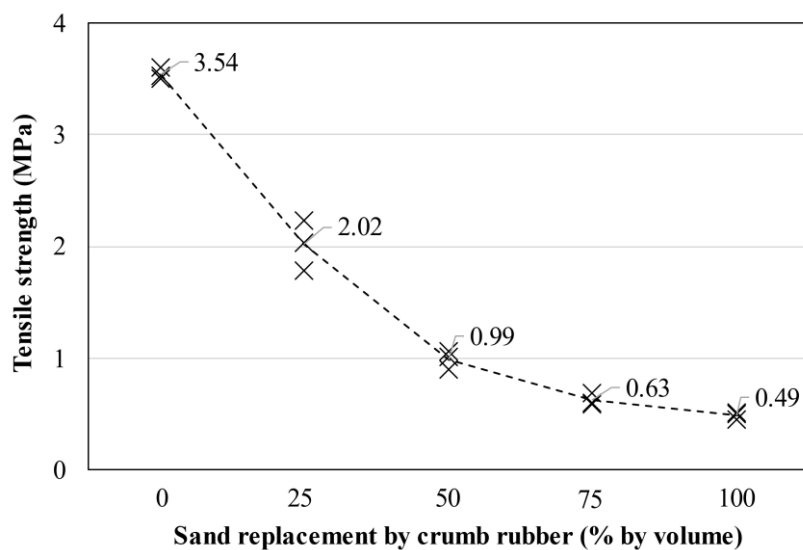

Figure 11. Tensile strength of cement mortar with crumb rubber

In this section, different amounts of crumb rubber were used to replace sand in the studied cement mortar samples to find the intrinsic mechanical properties of composites. It was found that the increased amount of sand replacement by crumb rubber reduced the unit weight, the compressive strength, the tensile strength, and the modulus of elasticity of the composite. These results of the mechanical properties of cement mortar with crumb rubber were subsequently used for the nonlinear analysis of reinforced concrete and crumb rubber mortar wall panels at the structural level.

3. Interaction of Reinforced Concrete Frame and Infill Wall Panel Under Lateral Load

In order to study the interaction between the reinforced concrete frame and the infilled wall panels made of cement mortar with crumb rubber under lateral load, a typical reinforced concrete frame with one bay and one story was selected with equivalent strut models representing the infill wall panel. Nonlinear frame analysis was performed, by using SAP2000 structural analysis software to investigate the interaction and lateral resisting mechanisms of the studied frame and the wall panel made of cement mortar with crumb rubber.

3.1. Typical Reinforced Concrete Frame with Infill Wall Panel

Figure 12 depicts the typical reinforced concrete frame with infill wall panels as common elements for residential low-rise buildings in Thailand. The center-to-center distance between the two columns was 4 meters, and the height between floors was 3.4 meters. Details of the columns and the beams are shown in Figure 13. The boundary conditions at the column bases were assumed to be fixed.
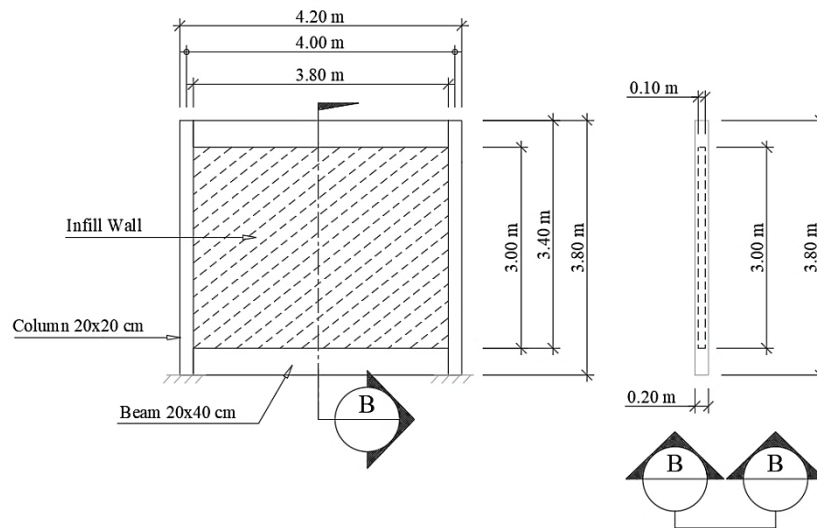

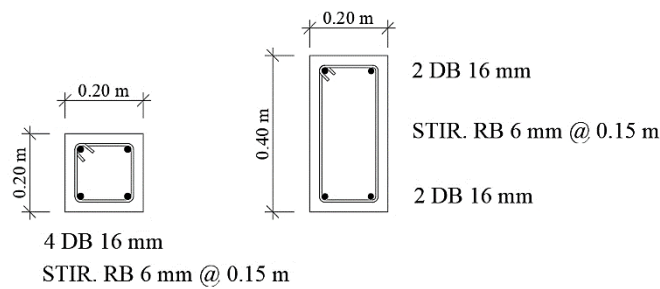**Figure 12. Reinforced concrete frame and infill wall model**

Figure 13. Details of columns and beams

The effective moment of inertia I_{eff} and the effective cross-sectional area A_{eff} of the beams and the columns were taken as follows:

Beam: $I_{eff} = 0.35 I_g$ (1)

Column: $I_{eff} = 0.70 I_g$ (2)

$A_{eff} = 1.0 A_g$ (3)

where I_g and A_g are the gross moment of inertia and the gross cross-sectional area, respectively.

For modeling the reinforced concrete frame, the concrete was assumed to have the compressive strength of 23.54 MPa, the modulus of elasticity of 22,979 MPa, the Poisson's ratio of 0.2 and the unit weight of 23.54 kN/m³. The longitudinal steel reinforcements were deformed bars with the yield strength of 392.4 MPa. The stirrups were round bars with the yield strength of 235.44 MPa. The infill wall panel was made of various mixes of cement mortar with crumb rubber, and their mechanical properties were determined using the test results presented in Section 2 of this paper.

3.2. Modelling of Infilled Wall Panel by Equivalent Compression Strut

The stress-strain relation of the cement mortar with crumb rubber in Figure 6 serves as a basis for model parameters of the equivalent compression strut to represent the behavior of the infill wall panel. To alleviate numerical issues that might arise during nonlinear incremental-iterative computation, the response of the equivalent compression strut was allowed to follow the adopted simplified tri-linear version of the stress-strain relation of cement mortar with crumb rubber, as illustrated in Figure 14. The simplified tri-linear stress-strain relation consists of four stress-strain coordinates; the first point corresponds to the origin, the second point is at $0.33 f'_{cm}$ of the wall panel, the third point is at f'_{cm}, and the fourth point is at the ultimate state corresponding to failure of the cement mortar specimens. The results of the simplified tri-linear stress-strain relation of the studied cement mortar with crumb rubber are presented in Table 2.
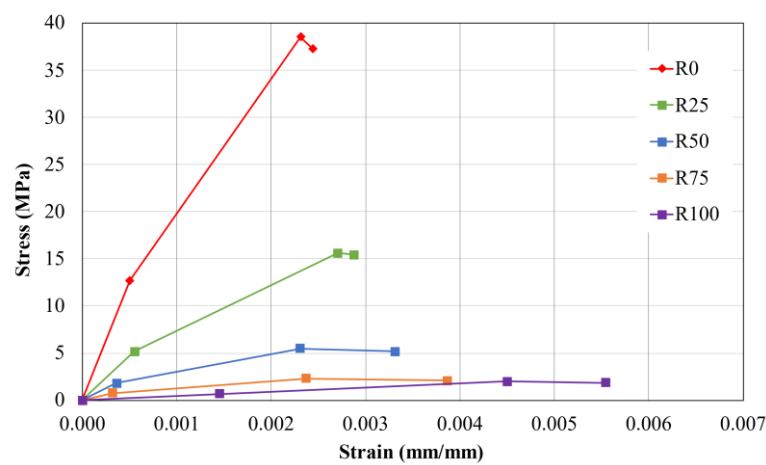

Figure 14. Simple stress-strain relation of the cement mortar specimens

Table 2. Simplified tri-linear stress-strain of cement mortar with crumb rubber

Point	R0		R25		R50		R75		R100	
	Stress (MPa)	Strain (-)	Stress (MPa)	Strain (-)	Stress (MPa)	Strain (-)	Stress (MPa)	Strain (-)	Stress (MPa)	Strain (-)
1	0.00	0.0000	0.00	0.0000	0.00	0.0000	0.00	0.0000	0.00	0.0000
2	12.70	0.0005	5.15	0.0006	1.82	0.0004	0.76	0.0003	0.65	0.0015
3	38.50	0.0023	15.60	0.0027	5.51	0.0023	2.30	0.0024	1.98	0.0045
4	37.28	0.0024	15.43	0.0029	5.18	0.0033	2.09	0.0039	1.87	0.0055

According to FEMA356 [33], the elastic in-plane stiffness of a solid unreinforced infill panel prior to cracking shall be represented by an equivalent diagonal compression strut of width, a, given:

$$a = 0.175(\lambda_1 h_{col})^{(-0.4)} r_{inf} \tag{4}$$

where λ_1 is the coefficient used to determine the equivalent strut width, in which;

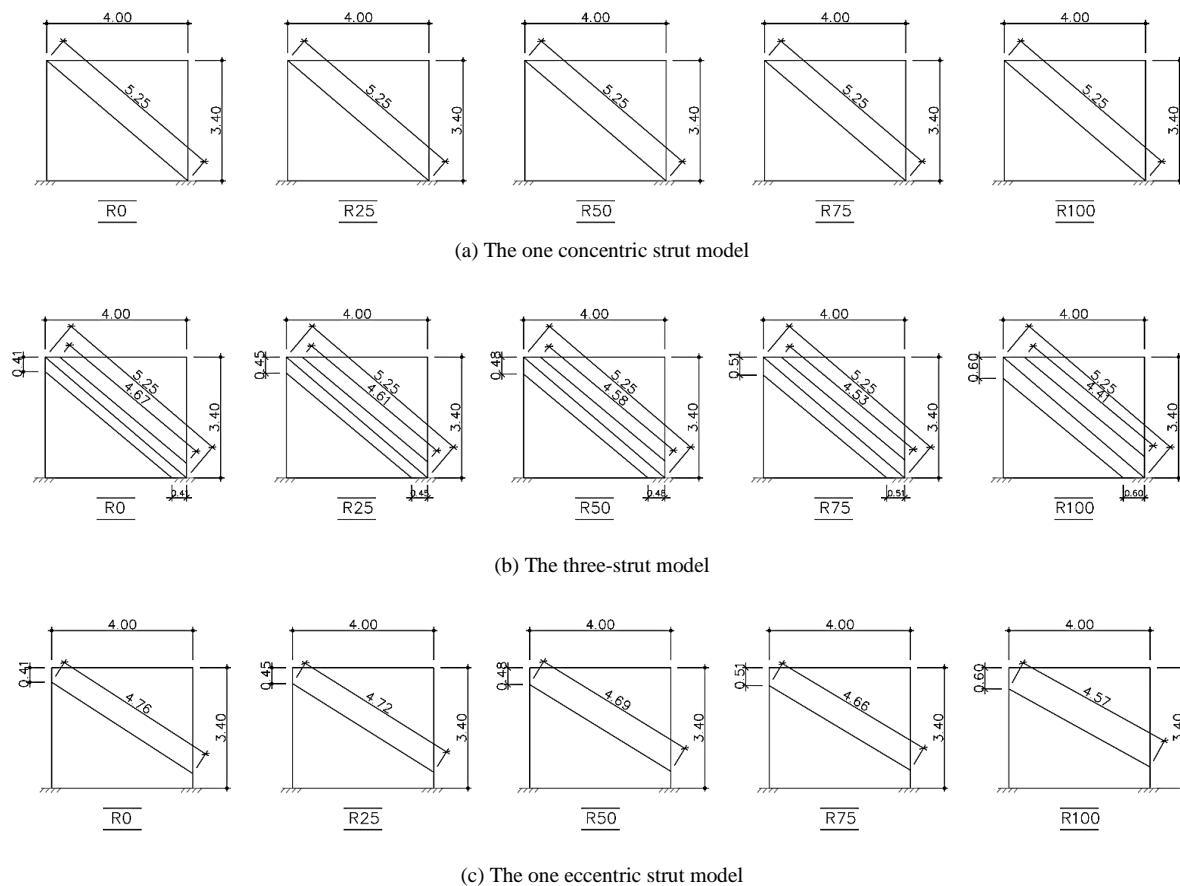$$\lambda_1 = [(E_{m_e} t_{inf} sin(2\theta))/(4 E_{fe} I_{col} h_{inf})]^{0.25} \tag{5}$$

where h_{col} is column height between centerlines of beams, h_{inf} is height of infill panel, E_{fe} is expected modulus of elasticity of frame, E_{m_e} expected modulus of elasticity of infill, I_{col} is moment of inertia of column, r_{inf} is diagonal length of infill panel, t_{inf} thickness of infill panel and equivalent strut, θ is angle whose tangent is the infill height-to-length aspect ratio.

In this study, it was assumed that the equivalent struts have the same thicknesses, and the modulus of elasticity follows the assumed tri-linear stress-strain relation of the cement mortar with crumb rubber as the infill panel. The parameters necessary for equivalent compressive strut modeling are summarized in Table 3.

Table 3. The parameters used to simulate equivalent compression strut

No.	Unit Weight (kN/m³)	Compressive Strength (MPa)	E_m (MPa)	λ_1	a (cm)	θ_c (degree)
R0	20.55	38.50	24,739.19	0.0031	32.95	36.77
R25	17.65	15.60	9,388.08	0.0024	36.30	36.40
R50	15.33	5.51	5,316.44	0.0021	38.42	36.17
R75	13.62	2.30	2,700.73	0.0018	41.12	35.87
R100	12.15	1.98	461.62	0.0012	49.06	35.00

To model the infill wall panel with crumb rubber, three equivalent compression strut models were applied. The details of the one concentric strut model, the three-strut model, and the one eccentric strut model are shown in Figures 15(a), 15(b), and 15(c), respectively. The overall strut widths in the three-strut model were the same as the width of the one strut in the one-strut models; the middle strut took half of the equivalent compression strut width, while each of the upper and lower struts took one-fourth of the width, according to [34].

(a) The one concentric strut model

(b) The three-strut model

(c) The one eccentric strut model

Figure 15. Details of the equivalent compression strut models

3.3. Modeling of Nonlinear Frame-Diagonal Compression Strut Interaction under Lateral Load

In accordance with [34, 37], the concept for nonlinear modeling of the frame-diagonal compression strut interaction under lateral load is shown in Figure 16. The interaction was analyzed by inclusion of flexural plastic hinges in the reinforced concrete frame allowing nonlinear moment-plastic rotation of the frame to develop. For the behavior of the reinforced concrete under flexural mode, the relation between moment-plastic rotation of the reinforced concrete frame herein was adopted based on ASCE41 guideline [32], as shown in Figure 17. For the behavior of the reinforced concrete frame under shear mode, the internal shear force developed in the frame was monitored and the frame was deemed to fail under shear when the shear force in the frame reached the shear capacity of the frame sections. For the given details of the columns, the nominal shear strength was 40 kN. For nonlinear modelling of the diagonal compression strut, an axial hinge was provided to capture the nonlinear stress-strain relation of the diagonal compression strut under lateral loading.
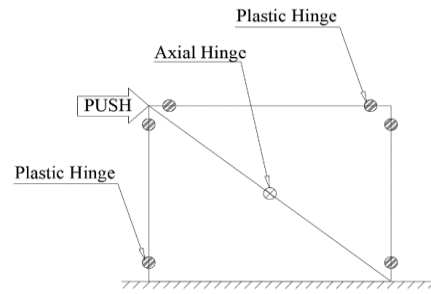
Figure 16. Concept for nonlinear modeling of frame-diagonal compression strut interaction by means of one diagonal equivalent strut representing wall panel
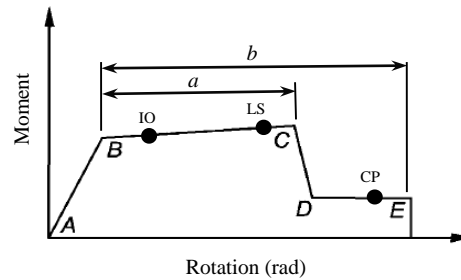

Figure 17. Moment-rotation relation of the studied columns of the frame

In this study, nonlinear incremental-iterative analysis of the frame-strut interaction was performed by displacement control of a control point. The nonlinear analysis was performed until failure, which could be in either the infill wall or the reinforced concrete frame.

3.4. Results of Reinforced Concrete Frame and Infilled Wall Panel under Lateral Load

The predicted relationships of lateral force and lateral displacement from the nonlinear frame-strut analyses using different diagonal compression strut concepts are shown in Figures 18–21. The results obtained by the one concentric strut model are shown in Figure 18. The response of the bare frame was observed to experience the plastic hinge formation of the column until the plastic rotation reached the level that triggered the collapse of some columns. The results revealed that inclusion of the wall panel in the frame analysis provided stiffer behavior and improved load capacity of the infilled frame in comparison with the bare frame. The amount of sand replacement by crumb rubber was shown to affect the flexibility of the infilled frame response. Using a greater amount of crumb rubber led to a more ductile frame response, whereas flexural hinge formation was observed at most of the hinges. The crushing failure of the strut was observed in all of the crumb-rubber-mixed specimens when the ultimate strain of the strut was reached prior to the failure in any of the reinforced concrete frame members. By using the one concentric strut model, it was observed in the R0 strut model that the lateral force acting on the infilled frame was dominantly resisted by the diagonal strut joining the column-beam joint and barely contributed by both columns of the frame, as shown in Figure 19. As such, the effect of the infilled wall-frame interaction on the columns of the frame cannot be explained by the one concentric strut model.
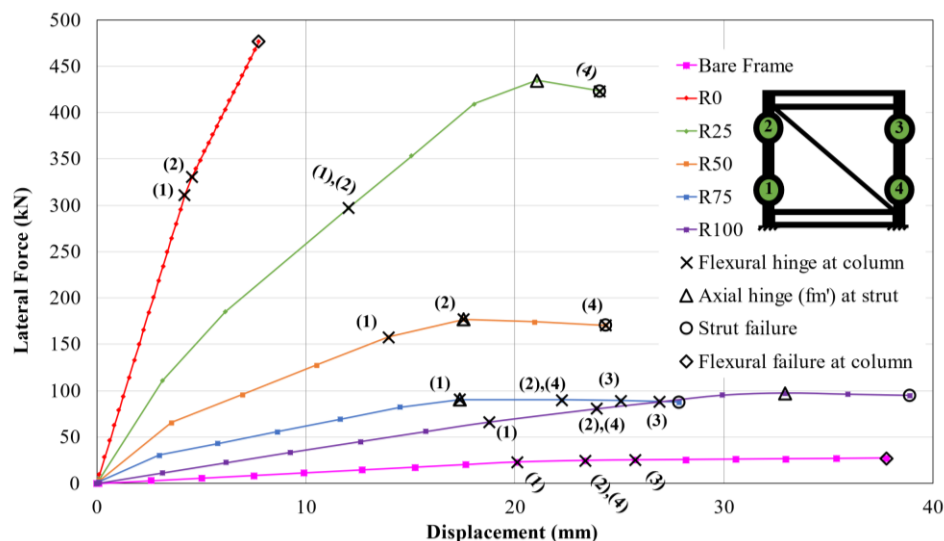

Figure 18. Relation between lateral force-displacement of the one concentric strut model
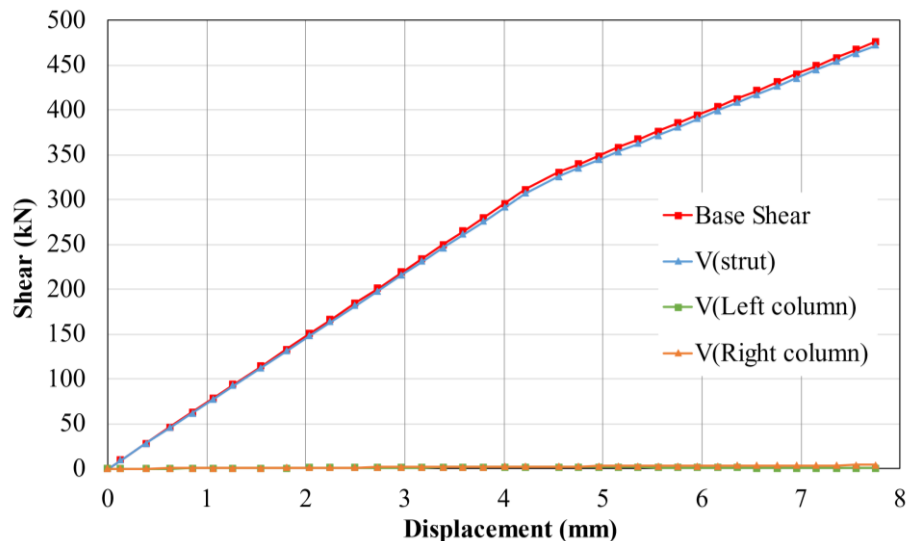
Figure 19. Internal shear distribution for case R0 by the one concentric strut model

The results obtained by the three-strut model are shown in Figure 20. The overall load capacity of the infilled frame in each case was regarded as more conservative in comparison with the results obtained by the one concentric strut model, in particular for the R0, R25, and R50 strut models. With the larger amount of crumb rubber, as in the R75 and R100 strut models, the infilled frame could undergo large deformation without the sign of failure in the columns. With less amount of crumb rubber, as in the R0, R25, and R50 strut models, the response of the infilled frame was not only stiffer, but it was also accompanied by the trigger of shear failure of the columns. It was noted that the deformation level at the shear failure of the columns was relevant to the amount of rubber inclusion. Increasing the amount of rubber inclusion could relatively improve the deformation ability of the infilled frame structure.
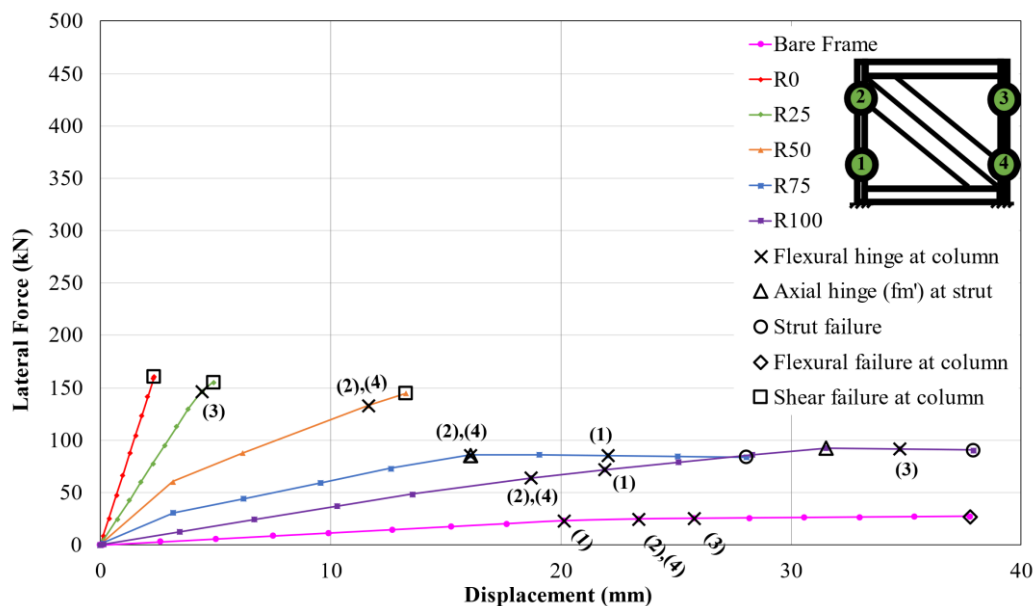

Figure 20. Relation between lateral force-displacement of the three-strut model

The overall load-displacement relation obtained using the one eccentric strut model is shown in Figure 21. With a larger amount of crumb rubber, the infilled frame could sustain much larger lateral deformation at approximately the same lateral peak load. It was observed that the failures of all the infilled frames were governed by shear failures in columns. The results obtained using the one eccentric strut model, in comparison with the other two models, could be considered the worst-case scenario, as shown in Figure 22. The predicted failure modes of the studied infill wall panel by various strut models are summarized in Table 4. In brief, inclusion of the wall panel in the nonlinear analysis resulted in stiffer responses than in the case of the solely bare reinforced concrete frame model. The presence of the wall panels within the frame could affect the deformation ability of the infilled frame in various ways.
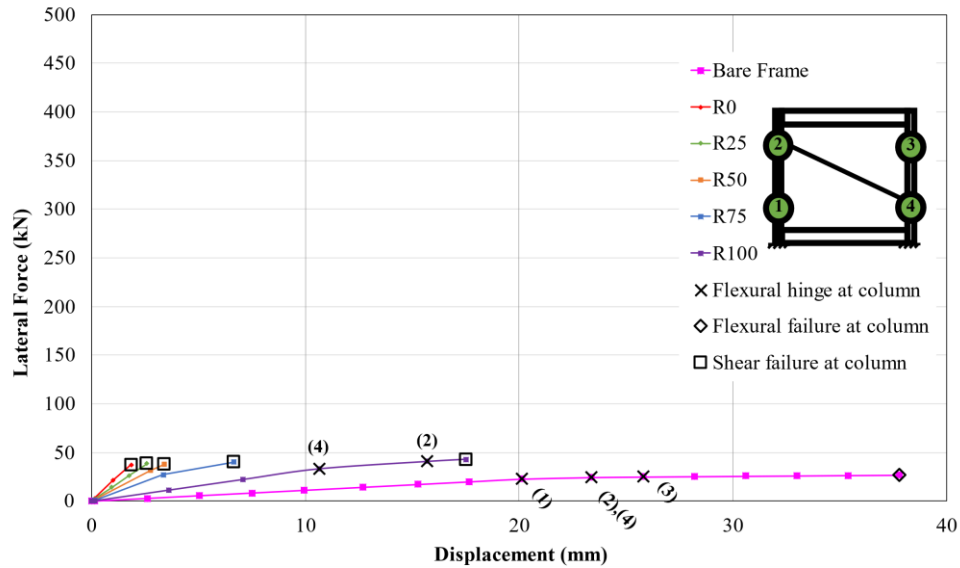
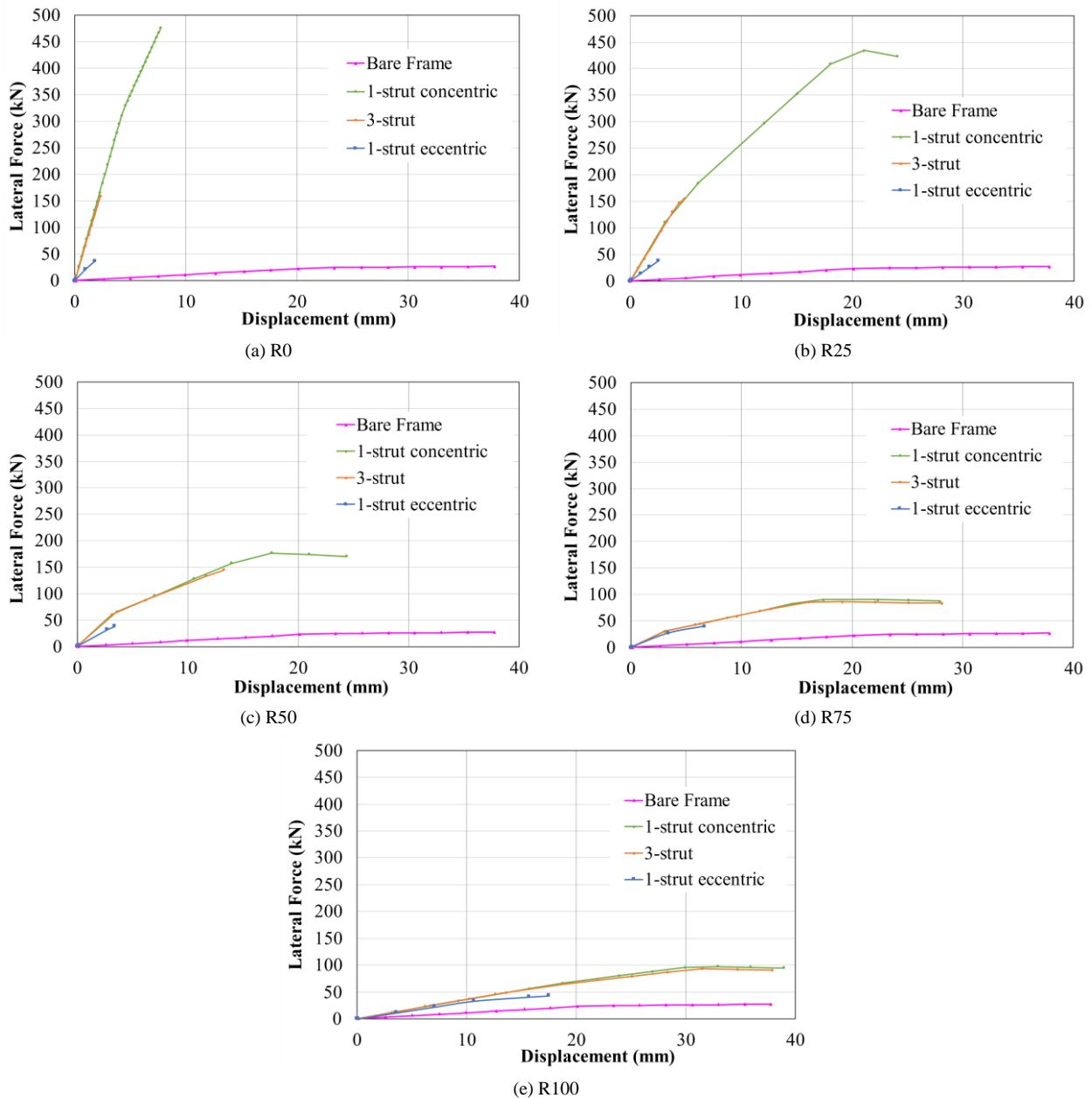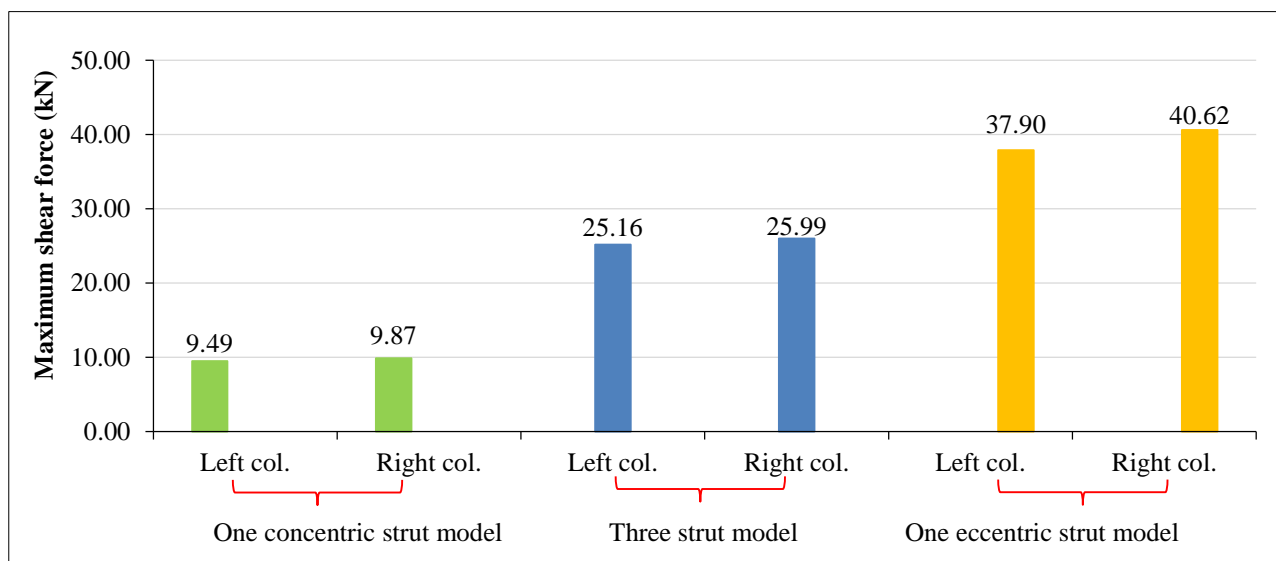**Figure 21. Lateral force-displacement relationship of the one eccentric strut model**

(a) R0

(b) R25

(c) R50

(d) R75

(e) R100

Figure 22. Lateral force-displacement relationships obtained by the strut models

Table 4. The predicted failure modes

No.	One concentric strut model		Three-strut model		One eccentric strut model	
	Failure mode	δ_y (mm)	**Failure mode**	δ_y (mm)	**Failure mode**	δ_y (mm)
R0	flexural failure at column	4.22	shear failure at column	N/A	shear failure at column	N/A
R25	strut failure	12.07	shear failure at column	4.41	shear failure at column	N/A
R50	strut failure	13.97	shear failure at column	11.67	shear failure at column	N/A
R75	strut failure	17.38	strut failure	16.07	shear failure at column	N/A
R100	strut failure	18.78	strut failure	18.73	shear failure at column	10.66

Adopting the one eccentric strut model for analysis of wall-frame interaction showed that the wall panel could interact with the columns by transferring the force into the columns of the infilled frame. The failure mode of the columns when interacting with the wall panel was different from the case of the bare frame, depending on the amount of crumb rubber used in the wall panel. The deformation ability of the infilled frame was less in comparison with the bare frame. The lateral displacement of the infilled frame when the column reached the effective yield point (equivalent to point B of the moment-rotation of Figure 17) is also collected in Table 4. When the shear failure was predicted to occur in a column that controlled the deformation ability of the infilled frame prior to flexural yielding of the column, no effective yield point of the column was reached. It was, however, noticed that the greater amount of rubber inclusion could relatively improve the deformation ability of the infilled frame. While the choice in adopting the strut modeling concept has still been an open issue [34, 45], the application of the one eccentric strut model has been recommended for evaluation of forces that may be imposed on the columns by the infill wall panel [32, 33]. The distribution of the lateral shear force in the columns is shown as an example in the case of the R75 strut model in Figure 23. The results from this study support the recommendation in [32, 33] that the one eccentric strut model can capture the interaction between the column and the wall more conservatively than the other two strut concepts.

Figure 23. The maximum shear forces in the left and the right columns at the final state of the R75 model

In this section, the load-deformation capacity curve of the reinforced concrete-infilled frame and crumb rubber mortar wall was studied. The influence of the mechanical properties of the cement mortar with crumb rubber on the lateral force-resisting mechanism between the infilled reinforced concrete frame and crumb rubber mortar wall panel was studied at the structural level. The present observations on the load-deformation capacity curve by using different diagonal strut modelings showed that the overall deformation ability of the reinforced concrete-infilled frame and wall was improved with higher percentages of the crumb rubber volume. The amount of used crumb rubber affected the stiffness of the crumb rubber mortar wall. With the higher percentages of crumb rubber volume, the ductility of the wall, as modeled by the diagonal strut, allowed for the higher deformation ability of the reinforced concrete-infilled frame and wall system. This interaction of the infilled crumb rubber mortar wall with the reinforced concrete frame under lateral load was affected by the compressive modulus of elasticity of the crumb rubber mortar. The compressive modulus was considered a key parameter affecting the behavior of the wall under compression, similar to the previous study [14]. This example reinforced concrete infilled frame and wall system was extended for the real-scale low-rise building in the next section to study the seismic performance of the infilled reinforced concrete frame with crumb rubber mortar at the real-scale building.

4. Seismic Performance of Example Building Frame with Infill Wall Panel

In this section, a simple building consisting of a regular frame and an infill wall panel was selected, as shown in Figure 24. The details of the beams and the columns were identical to those of the typical frame outlined in the previous section. The objective of this section is to investigate the potential seismic performance of the example building frame with a wall panel made of cement mortar with crumb rubber of different unit weights and different modulus of elasticity.
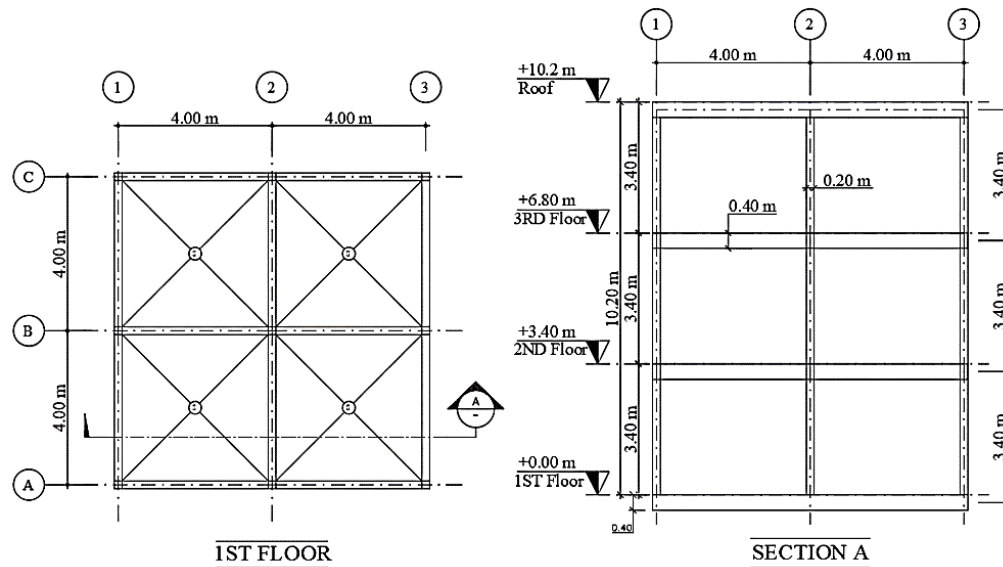

Figure 24. Details of the studied building

4.1. Details of Example Building

The example building was treated as an ordinary moment-resisting frame consisting of two bays and three stories. The building was located in Chiang Khan District, Loei Province, Thailand. It was assumed that the building was placed on normal soil layers. The design earthquake, for which its intensity level is two thirds of the maximum considered earthquake following the Thai standards DPT1301/1302-61 [41], was adopted. The spectral acceleration at structural period of 0.2 second (S_s) was taken as 0.265g. The spectral acceleration at structural period of 1 second (S_1) was taken as 0.066g. The equivalent static approach was adopted with the natural period of the studied building being 0.204 second and the design spectral acceleration (S_a) being 0.28g. The response modification factor (R) was taken as 3. This building was not designed to withstand earthquakes in the past and deemed as one of the typical existing low-rise buildings before Thailand issued a legal design regulation for buildings located in seismic zones in the year 2021 [41].

The main reinforced concrete frame on grid line B was chosen for analysis. A unit weight of 23.54 kN/m^3 was used for the cast-in-place reinforced concrete column, beams, and precast concrete slabs. It was assumed that the frames were equipped with a full infill wall with no openings. The R0, R25, R50, R75, and R100 wall panels were applied. For comparison with general practice in Thailand, infill walls made of clay bricks and autoclaved aerated concrete blocks were also considered, while no live load was considered. The total dead weight and seismic base shear for the sample building frames with different wall materials are summarized in Table 5. It is noted that the wall weight imposed by the clay brick panel was approximately 95% of the wall weight imposed by the R0 panel, whereas the wall weight imposed by the autoclaved aerated concrete block panel was around 80% of the wall weight imposed by the R100 wall panel. The various levels of crumb rubber inclusion in the wall panels yielded the different total dead weights for the building, as shown in Figure 25. With less weight in the building, the seismic base shear induced in the frame of grid line B was less demanding, as shown in Figure 26.

Table 5. Total weight and base shear of the example building using different wall system

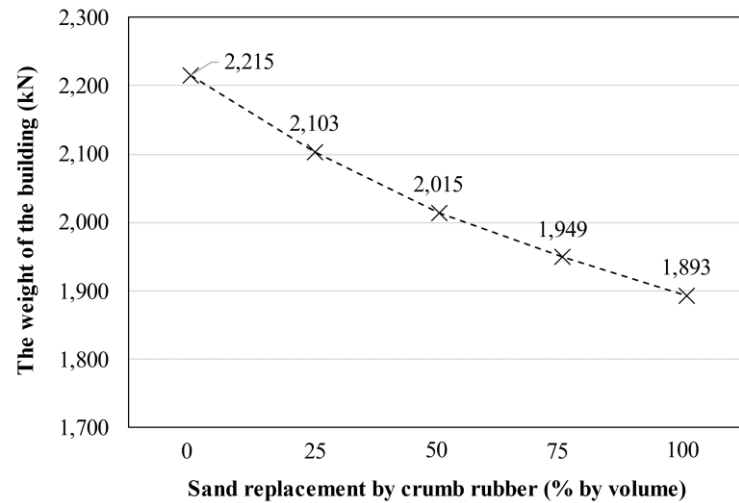| Type	R0	R25	R50	R75	R100	Clay brick	Autoclaved aerated concrete
Column	86.45	86.45	86.45	86.45	86.45	86.45	86.45
Beam	361.64	361.64	361.64	361.64	361.64	361.64	361.64
Floor	979.43	979.43	979.43	979.43	979.43	979.43	979.43
Wall	787.00	675.92	587.14	521.63	465.35	751.52	375.76
Total weight, W (kN)	2,214.52	2,103.44	2,014.66	1,949.15	1,892.87	2,179.04	1,803.28
Base Shear, V (kN)	265.74	252.41	241.76	233.90	227.14	261.49	216.39

Figure 25. The weight of the building imposed on the frame of grid line B
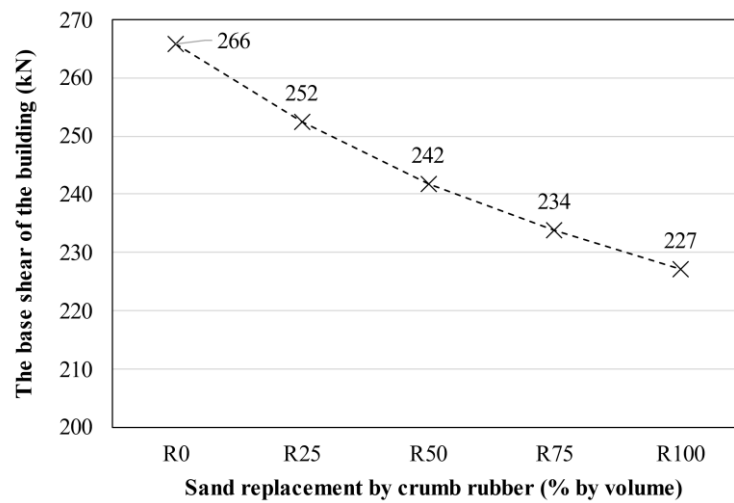

Figure 26. The base shear of the building imposed on the frame of grid line B

4.2. Influence of Crumb Rubber on Seismic Building Performance

The seismic analysis of the example building was performed by using the equivalent static approach [41], in which the seismic base shear was distributed at each floor level of the frame. The eccentric strut model in the previous section was used for the infilled frames, the details of which are shown in Figure 27. Although the bare frame analysis did not include the wall model itself, the dead weight of the walls and the associated induced seismic base shear were directly included in the analysis for comparison.
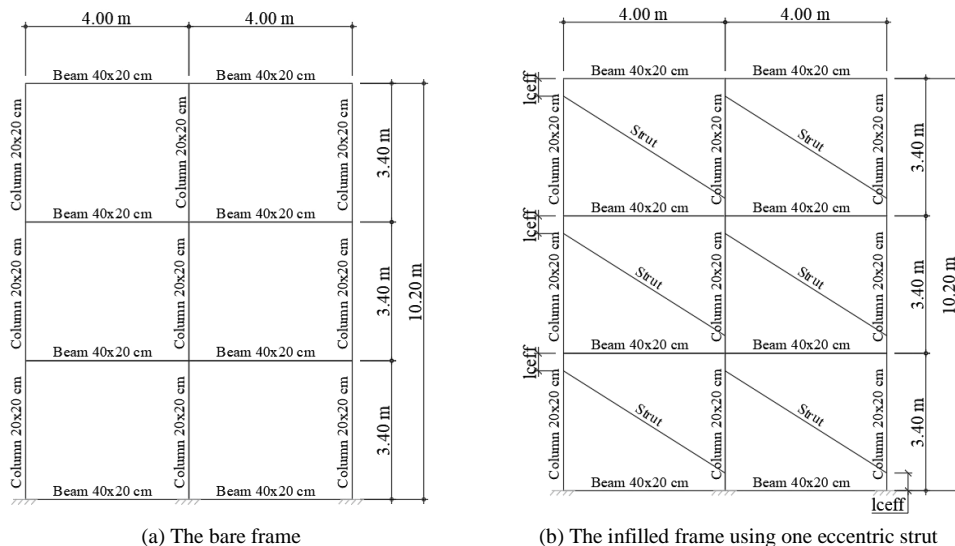

(a) The bare frame   (b) The infilled frame using one eccentric strut

Figure 27. The frame modeling

4.2.1. Seismic Force Demand in The Columns

For the moment-resisting building frame system, the lateral load was resisted mainly by the columns of the buildings. For the example building, the columns had the nominal shear strength (V_n) of 40 kN and the nominal moment strength (M_n) of 22 kN-m. Figure 28 shows the internal shear force demand (V_u) to shear capacity (V_n) ratio of a critical column located on the first story, based on different levels of crumb rubber inclusion in the wall panel. With the eccentric strut model, the predicted internal shear force induced in the column was greater than the result obtained by the bare frame analysis. With a greater amount of crumb rubber in the wall panel, the building weight as well as the V_u/V_n ratio were decreased in both the bare frame and infilled frame. Figure 29 shows the internal bending moment demand (M_u) to nominal moment strength (M_n) ratio of the same critical column, obtained by using different models. The struts were predicted to behave elastically based on the observed axial stress in the struts, as summarized in Figure 30. The predicted internal bending moment in the column was less using the eccentric strut model than the bare frame analysis. This implied that the wall-frame interaction might assist in reducing the amount of bending moment in the column, which was contrary to the increasing shear. It was noted that, without including the infill wall model in the bare frame analysis, the flexural demand of the column was lowered for a greater amount of crumb rubber in the wall panel. However, the change in the flexural demand of the critical column might not be obviously seen from the infilled frame analysis of the example building.
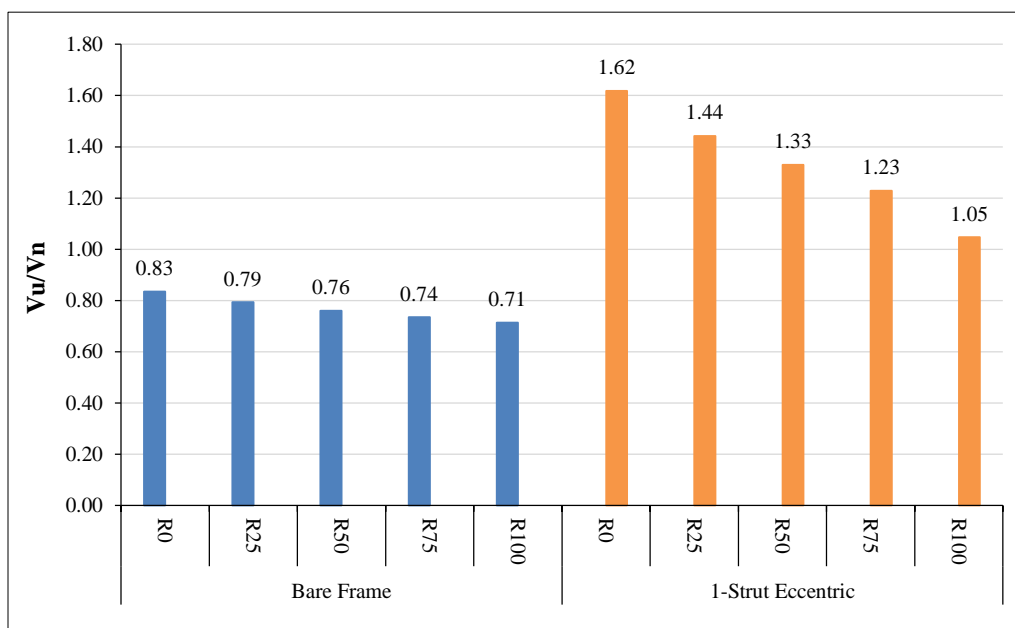

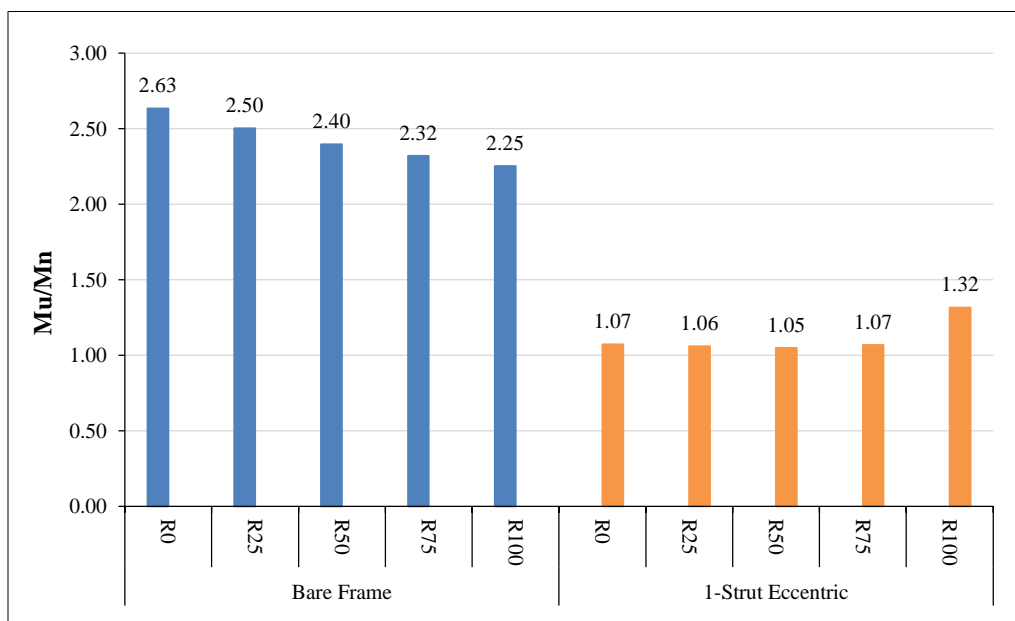**Figure 28. Comparison of V_u/V_n obtained from the model**

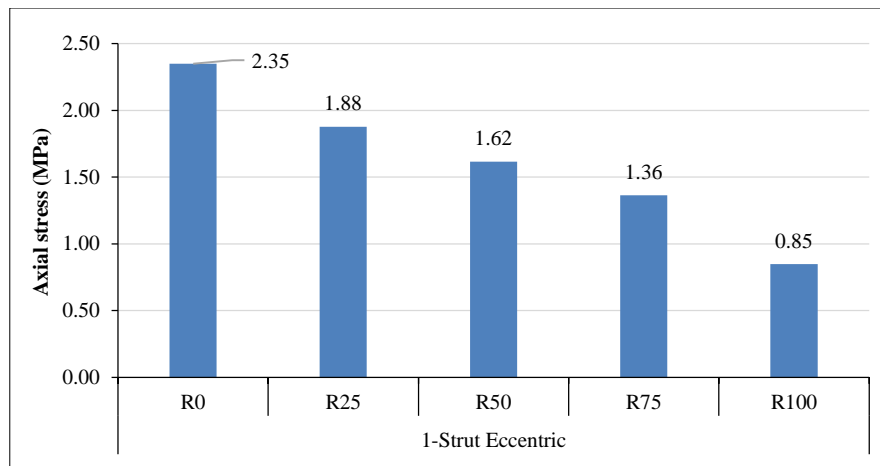**Figure 29. Comparison of M_u/M_n obtained from the model**

Figure 30. Axial stress of compression strut

4.2.2. Inter-Story Drift of The Example Building

The inter-story drifts along the height of the bare frame and the infilled frame are shown in Figure 31. It was found that the inter-story drift of the bare frame model was significantly greater than that of the infilled frame analyses. The maximum values of the inter-story drifts are summarized in Figure 32. It was observed that the inter-story drifts were reduced by infill wall-frame interaction. For the example building, the maximum story drift was observed to take place at the second-floor level of the frame. The maximum inter-story drift was increased with the increased rubber inclusion. According to ASCE 41, the magnitude of the inter-story drift can be related to the structural integrity of the structure. For the chosen building site of the study, the application of crumb rubber resulting in the maximum inter-story drift was less than 1.00% which was the threshold to ensure the life safety performance requirement.
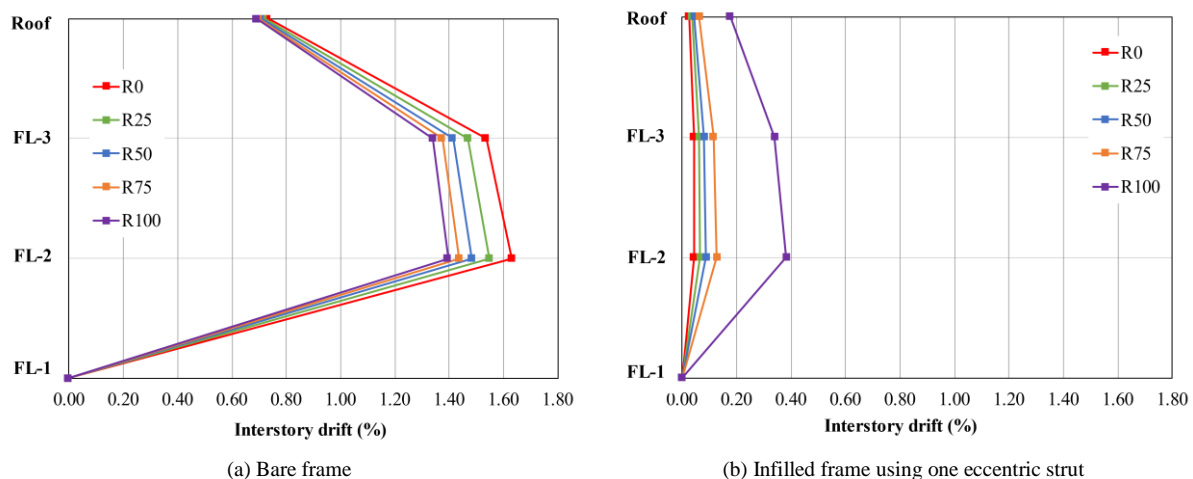

(a) Bare frame

(b) Infilled frame using one eccentric strut

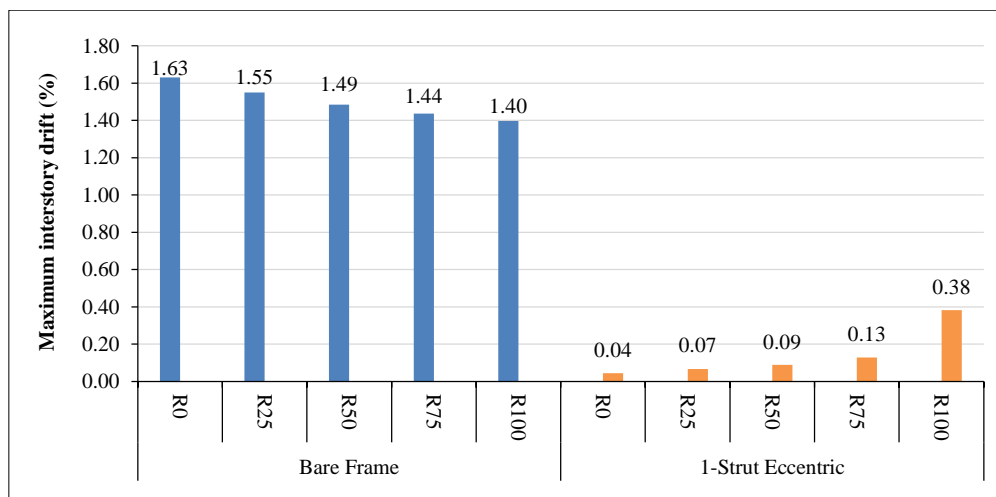**Figure 31. Inter-story drifts of the example building**

Figure 32. Maximum inter-story drift of the example building

In this section, the seismic performance of the building-scale infilled reinforced concrete frame with a crumb rubber mortar wall was studied. The use of crumb rubber in crumb rubber mortar walls resulted in less dead load on the wall imposed on the building frame. The analysis showed that the additional internal shear force induced in the infilled reinforced concrete frame can be reduced depending on the amount of crumb rubber. The observed inter-story drift of the present studied building did not exceed the level of life safety performance. This study demonstrated that the seismic performance of the building could be improved by the approach of lowering seismic demand through the use of lighter and more flexible crumb rubber mortar wall panels.

5. Conclusions

In this research, the engineering issues for the future use of crumb rubber to make non-structural wall panels are explored. The investigation is made for the possible lateral interaction of the infill wall and the frame and its effect on the seismic performance of the example building. The following conclusions can be drawn:

- The experiment to determine the mechanical properties of cement mortar with sand replacement by crumb rubber is conducted. The amounts of sand replacement by crumb rubber in this study are taken as 0, 25, 50, 75, and 100 percent by volume. It is found that the unit weight, the compressive strength, the tensile strength, and the modulus of elasticity decrease with an increased amount of crumb rubber. The unit weights are in the range of 12–21 kN/m^3. The compressive strengths at 28 days are in the range of 2–28 MPa. The tensile strengths at 28 days are in the range of 0.5–3.5 MPa, accounting for 9–25 percent of the compressive strength. The moduli of elasticity are in the range of 462–24,739 MPa. The Poisson's ratios are in the range of 0.19–0.22.

- Based on the properties of various mixes of cement mortar with crumb rubber, nonlinear analyses of infilled frames are performed by using SAP2000 program. Based on three equivalent compression strut concepts, force interaction between the wall panel and the columns can be most conservatively captured by using the one eccentric strut concept. The deformation ability of the infilled frame is different from the bare frame itself. The inclusion of the wall panel can trigger a different mode of failure in columns. Column shear failure mode can be observed for the infilled frame response, while the bare frame response is controlled by column flexural bending. The deformation ability of the infilled frame is shown to be improved with the increased crumb rubber inclusion in the wall panel.

- Based on the example building frame, seismic analysis by the equivalent static approach is carried out. It is shown that the seismic performance of the building that includes the wall panels in the structural model is different from the building performance predicted merely by the bare frame analysis itself. The shear force prediction in the columns is more conservative when modeling the wall panel using the one eccentric strut concept. The maximum inter-story drift of the building frame is reduced with the inclusion of the wall panels. Using the infill wall with a higher amount of crumb rubber can decrease the weight of the building. As a result, the seismic demands, i.e., internal shear force and bending moment induced in the columns, are less despite being accompanied by higher inter-story drift for the chosen building.

This paper demonstrates an evaluation example of the seismic performance of the building frame with the selected crumb rubber mortar, the chosen geometry and size of the wall, and the building frame. The process can be extended to cover different crumb rubber mortar and/or concrete compositions, as well as different building types. With a better understanding of the interaction between crumb rubber wall and building structure, the efficient design and use of crumb rubber mortar wall in the building can be optimized for future work with the recently proposed environmental viability analysis for crumb rubber mortar application in construction [46].

6. Declarations

6.1. Author Contributions

Conceptualization, M.B. and T.P.; methodology, M.B. and T.P.; validation, M.B.; investigation, K.C.; writing—original draft preparation, K.C. and M.B.; writing—review and editing, M.B., T.P., V.S., and C.C.; supervision, M.B. All authors have read and agreed to the published version of the manuscript.

6.2. Data Availability Statement

The data presented in this study are available on request from the corresponding author.

6.3. Funding

6.4. Conflicts of Interest

The authors declare no conflict of interest.

7. References

[1] Fazli, A., & Rodrigue, D. (2020). Recycling waste tires into ground tire rubber (GTR)/rubber compounds: A review. Journal of Composites Science, 4(3), 103. doi:10.3390/jcs4030103.

[2] Nadal, M., Rovira, J., Díaz-Ferrero, J., Schuhmacher, M., & Domingo, J. L. (2016). Human exposure to environmental pollutants after a tire landfill fire in Spain: Health risks. Environment International, 97, 37–44. doi:10.1016/j.envint.2016.10.016.

[3] Sidhu, K. S., Keeslar, F. L., & Warner, P. O. (2006). Potential health risks related to tire fire smoke. Toxicology International, 13(1), 1–17.

[4] Rogachuk, B. E., & Okolie, J. A. (2023). Waste tires based biorefinery for biofuels and value-added materials production. Chemical Engineering Journal Advances, 14, 100476. doi:10.1016/j.ceja.2023.100476.

[5] Valentini, F., & Pegoretti, A. (2022). End-of-life options of tyres. A review. Advanced Industrial and Engineering Polymer Research, 5(4), 203–213. doi:10.1016/j.aiepr.2022.08.006.

[6] Khaloo, A. R., Dehestani, M., & Rahmatabadi, P. (2008). Mechanical properties of concrete containing a high volume of tire-rubber particles. Waste Management, 28(12), 2472–2482. doi:10.1016/j.wasman.2008.01.015.

[7] Gupta, T., Chaudhary, S., & Sharma, R. K. (2016). Mechanical and durability properties of waste rubber fiber concrete with and without silica fume. Journal of Cleaner Production, 112, 702–711. doi:10.1016/j.jclepro.2015.07.081.

[8] Sofi, A. (2018). Effect of waste tyre rubber on mechanical and durability properties of concrete – A review. Ain Shams Engineering Journal, 9(4), 2691–2700. doi:10.1016/j.asej.2017.08.007.

[9] Liu, H., Wang, X., Jiao, Y., & Sha, T. (2016). Experimental investigation of the mechanical and durability properties of crumb rubber concrete. Materials, 9(3), 172. doi:10.3390/ma9030172.

[10] Chen, H., Li, D., Ma, X., Zhong, Z., & Abd-Elaal, E. S. (2023). Compressive strength prediction of crumb rubber mortar based on mesoscale model. Engineering Failure Analysis, 152, 107485. doi:10.1016/j.engfailanal.2023.107485.

[11] Wongsa, A., Sata, V., Nematollahi, B., Sanjayan, J., & Chindaprasirt, P. (2018). Mechanical and thermal properties of lightweight geopolymer mortar incorporating crumb rubber. Journal of Cleaner Production, 195, 1069–1080. doi:10.1016/j.jclepro.2018.06.003.

[12] Shahrul, S., Mohammed, B. S., Wahab, M. M. A., & Liew, M. S. (2021). Mechanical properties of crumb rubber mortar containing nano-silica using response surface methodology. Materials, 14(19), 5496. doi:10.3390/ma14195496.

[13] Sukontasukkul, P. (2009). Use of crumb rubber to improve thermal and sound properties of pre-cast concrete panel. Construction and Building Materials, 23(2), 1084–1092. doi:10.1016/j.conbuildmat.2008.05.021.

[14] Al-Fakih, A., Mohammed, B. S., Al-Osta, M. A., & Assaggaf, R. (2022). Evaluation of the mechanical performance and sustainability of rubberized concrete interlocking masonry prism. Journal of Materials Research and Technology, 18, 4385–4402. doi:10.1016/j.jmrt.2022.04.115.

[15] Bewick, B. T., Salim, H., Saucier, A., & Jackson, C. (2010). Crumb rubber-concrete panels under blast loads. Air Force Research Laboratory, Materials and Manufacturing Directorate, 1-14.

[16] Naito, C., States, J., Jackson, C., & Bewick, B. (2014). Assessment of Crumb Rubber Concrete for Flexural Structural Members. Journal of Materials in Civil Engineering, 26(10), 04014075. doi:10.1061/(asce)mt.1943-5533.0000986.

[17] Rigotti, D., & Dorigato, A. (2022). Novel uses of recycled rubber in civil applications. Advanced Industrial and Engineering Polymer Research, 5(4), 214–233. doi:10.1016/j.aiepr.2022.08.005.

[18] Wararuksajja, W., Srechai, J., Leelataviwat, S., Sungkamongkol, T., & Limkatanyu, S. (2021). Seismic design method for preventing column shear failure in reinforced concrete frames with infill walls. Journal of Building Engineering, 44, 102963. doi:10.1016/j.jobe.2021.102963.

[19] Crisafulli, F. J. (1997). Seismic behavior of reinforced concrete structures with masonry infills. PhD Thesis., University of Canterbury Christchurch, Christchurch, New Zealand.

[20] Angel, R. (1994). Behavior of reinforced concrete frames with masonry infills. Ph.D. Thesis, University of Illinois Urbana-Champaign, Champaign–Urbana, USA.

[21] Netrattana, C. (2013). Evaluation of reinforced concrete buildings under earthquakes considering effects of masonry infills. Ph.D. Thesis, Chulalongkorn University, Bangkok, Thailand. doi:10.14457/CU.the.2013.1347.

[22] Khan, N. A., Monti, G., Nuti, C., & Vailati, M. (2021). Effects of infills in the seismic performance of an RC factory building in Pakistan. Buildings, 11(7), 276. doi:10.3390/buildings11070276.

[23] Okail, H., Abdelrahman, A., Abdelkhalik, A., & Metwaly, M. (2016). Experimental and analytical investigation of the lateral load response of confined masonry walls. HBRC Journal, 12(1), 33–46. doi:10.1016/j.hbrcj.2014.09.004.

[24] Mehrabi, A. B., Benson Shing, P., Schuller, M. P., & Noland, J. L. (1996). Experimental Evaluation of Masonry-Infilled RC Frames. Journal of Structural Engineering, 122(3), 228–237. doi:10.1061/(asce)0733-9445(1996)122:3(228).

[25] Mahmud, E., Bonev, Z., & Abdulahad, E. (2019). Nonlinear seismic analysis of masonry infilled RC frame structures. Gradjevinski Materijali i Konstrukcije, 62(1), 17–25. https://doi.org/10.5937/grmk1901017m.

[26] Grubišić, M., Kalman Šipoš, T., Grubišić, A., & Pervan, B. (2023). Testing of Damaged Single-Bay Reinforced Concrete Frames Strengthened with Masonry Infill Walls. Buildings, 13(4), 1021. doi:10.3390/buildings13041021.

[27] Teguh, M. (2017). Experimental Evaluation of Masonry Infill Walls of RC Frame Buildings Subjected to Cyclic Loads. Procedia Engineering, 171, 191–200. doi:10.1016/j.proeng.2017.01.326.

[28] Ozyurt, M. Z., & Almannaa, W. (2024). Effect of modelling the infill wall as a strut element on the structure behaviour. Journal of Radiation Research and Applied Sciences, 17(1), 100755. doi:10.1016/j.jrras.2023.100755.

[29] Wararuksajja, W., Srechai, J., & Leelataviwat, S. (2020). Seismic design of RC moment-resisting frames with concrete block infill walls considering local infill-frame interactions. Bulletin of Earthquake Engineering, 18(14), 6445–6474. doi:10.1007/s10518-020-00942-9.

[30] Tanjung, J., Ismail, F. A., Maidiawati, Nur, O. F., & Mahlil. (2019). Experimental study for evaluating the seismic performance of RC frame structure with partially infilled by brick masonry. International Journal of GEOMATE, 16(57), 189–194. doi:10.21660/2019.57.8340.

[31] Constantinescu, S. (2021). Study on the behavior of a high reinforced concrete building with different kinds of partitioning masonry walls. IOP Conference Series: Earth and Environmental Science, 664(1), 12050. doi:10.1088/1755-1315/664/1/012050.

[32] ASCE/SEI41-17. (2017). Seismic Evaluation and Retrofit of Existing Buildings. American Society of Civil Engineers (ASCE), Reston, United States. doi:10.1061/9780784414859.

[33] FEMA 356. (2000). Prestandard and commentary for the seismic rehabilitation of buildings. Federal Emergency Management Agency (FEMA), Washington, United States.

[34] Crisafulli, F. J., & Carr, A. J. (2007). Proposed macro-model for the analysis of infilled frame structures. Bulletin of the New Zealand Society for Earthquake Engineering, 40(2), 69–77. doi:10.5459/bnzsee.40.2.69-77.

[35] Srechai, J., Leelataviwat, S., Wararuksajja, W., & Limkatanyu, S. (2022). Multi-strut and empirical formula-based macro modeling for masonry infilled RC frames. Engineering Structures, 266, 114559. doi:10.1016/j.engstruct.2022.114559.

[36] Roosta, S., & Liu, Y. (2022). Development of a Macro-Model for concrete masonry infilled frames. Engineering Structures, 257, 114075. doi:10.1016/j.engstruct.2022.114075.

[37] Van, T. C., Lau, T. L., & Mohamed Nazri, F. (2022). Macro-modeling approach incorporating fiber plastic hinge for reinforced concrete frames with masonry infill. Engineering Structures, 251, 113421. doi:10.1016/j.engstruct.2021.113421.

[38] Crisafulli, F. J., Carr, A. J., & Park, R. (2000). Analytical modelling of infilled frame structures - A general review. Bulletin of the New Zealand Society for Earthquake Engineering, 33(1), 30–47. doi:10.5459/bnzsee.33.1.30-47.

[39] Smyrou, E., Blandon, C., Antoniou, S., Pinho, R., & Crisafulli, F. (2011). Implementation and verification of a masonry panel model for nonlinear dynamic analysis of infilled RC frames. Bulletin of Earthquake Engineering, 9(5), 1519–1534. doi:10.1007/s10518-011-9262-6.

[40] Bourahla, N. (2015). Equivalent Static Analysis of Structures Subjected to Seismic Actions. Encyclopedia of Earthquake Engineering, Springer, Berlin, Germany. doi:10.1007/978-3-642-35344-4_169.

[41] DPT 1301/1302-61. (2018). Earthquake Resistant Design code DPT 1301/1302-61. Department of Public Works and Town & Country Planning, Ministry of Interior, Bangkok, Thailand.

[42] ASTM C109/C109M-01. (2017). Standard Test Method for Compressive Strength of Hydraulic Cement Mortars (Using 2-in. or [50-mm] Cube Specimens). ASTM International, Pennsylvania, United States. doi:10.1520/C0109_C0109M-01.

[43] ASTM C192/C192M-19. (2020). Standard Practice for Making and Curing Concrete Test Specimens in the Laboratory. ASTM International, Pennsylvania, United States. doi:10.1520/C0192_C0192M-19.

[44] TMS 402/602-16. (2016). Building Code Requirements for Masonry Structures. The Masonry Society, Longmont, United States.

[45] Falcão Moreira, R., Varum, H., & Castro, J. M. (2023). Influence of Masonry Infill Walls on the Seismic Assessment of Non-Seismically Designed RC Framed Structures. Buildings, 13(5). doi:10.3390/buildings13051148.

[46] Los Santos - Ortega, J., Fraile - García, E., & Ferreiro - Cabello, J. (2023). Methodology for the environmental analysis of mortar doped with crumb rubber from end-of-life tires. Construction and Building Materials, 399, 132519. doi:10.1016/j.conbuildmat.2023.132519.